Effect of pressure on electronic and thermoelectric properties of magnesium silicide: A density functional theory study*

Kulwinder Kaur† and Ranjan Kumar

Department of Physics, Panjab University, Chandigarh-160014, India

(Received 21 December 2015; revised manuscript received 15 January 2016; published online 31 March 2016)

We study the effect of pressure on electronic and thermoelectric properties of Mg_2Si using the density functional theory and Boltzmann transport equations. The variation of lattice constant, band gap, bulk modulus with pressure is also analyzed. Further, the thermoelectric properties (Seebeck coefficient, electrical conductivity, electronic thermal conductivity) have been studied as a function of temperature and pressure up to 1200 K. The results show that Mg_2Si is an n-type semiconductor with a band gap of 0.21 eV. The negative value of the Seebeck coefficient at all pressures indicates that the conduction is due to electrons. With the increase in pressure, the Seebeck coefficient decreases and electrical conductivity increases. It is also seen that, there is practically no effect of pressure on the electronic contribution of thermal conductivity. The paper describes the calculation of the lattice thermal conductivity and figure of merit of Mg_2Si at zero pressure. The maximum value of figure of merit is attained 1.83×10^{-3} at 1000 K. The obtained results are in good agreement with the available experimental and theoretical results.

Keywords: semiconductors, effects of pressure, electric and thermal conductivity, density functional theory

PACS: 64.70.kg, 74.62.Fj, 74.25.fc, 71.15.Mb **DOI:** 10.1088/1674-1056/25/5/056401

1. Introduction

Thermoelectric based generators and refrigerators are solid-state devices in which heat energy is converted into electricity and vice versa. Thermoelectric generators have been used in power generation and remote power sources.[1] Thermoelectric generators are noiseless, reliable, and have no moving parts. Now, these generators are used in aerospace and military applications. Several thermoelectric materials based on tellurium, lead, antimony, and selenium has been investigated. These materials are more efficient because of high figure of merit, but are not safe to handle because of their toxic nature. These materials are less abundant and more expensive. Thus, it is a great challenge to search for new thermoelectric materials that are low cost, non toxic, and environment friendly. Semiconducting alkaline earth metal silicides have been of great interest due to their applications in thermoelectric devices.[2,3] Magnesium silicide and related alloys are promising material for thermoelectric devices because of their non toxic nature, thermal stability, low density, relative abundance, and low cost of production. Mg_2Si material has been considered as a high performance thermoelectric material in the temperature range of 500 K–800 K.[4,5] Due to high specific strength and elastic modulus, Mg_2Si can be used in the automobile and aerospace industry.[6,7] This material can also be used for optical fibers because it has good ohmic contact with Si.[8] Magnesium silicide is an n-type semiconductor having a band gap of 0.37 eV–0.78 eV.[9,10]

The parameter which evaluates the performance of thermoelectric materials is a dimensionless figure of merit ZT,[11] which is defined as

$$\mathrm{ZT} = \frac{S^2\sigma T}{k}, \tag{1}$$

where S, σ, k, and T are Seebeck coefficient, electrical conductivity, thermal conductivity, and temperature, respectively. Further, the product of the Seebeck coefficient and electrical conductivity is known as thermopower ($S^2\sigma$). The efficiency η[12] of any thermoelectric generator or refrigerator depends upon ZT as a given below

$$\eta = \frac{T_\mathrm{H} - T_\mathrm{C}}{T_\mathrm{H}} \frac{\sqrt{1+\mathrm{ZT}} - 1}{\sqrt{1+\mathrm{ZT}} + \dfrac{T_\mathrm{C}}{T_\mathrm{H}}}, \tag{2}$$

where T_H and T_C refer to the temperature of the hot and cold sides of the sample, respectively.

Efficient thermoelectric materials have high thermopower and low thermal conductivity. High performance thermoelectric materials have ZT equal to or greater than one. Baranek *et al.*[13,14] reported electronic, elastic, and phonon properties of this compound at zero pressure. Their studies have shown that the band gap is greater than the experimental value and all the electron calculations point out a mixed ionic–covalent nature of Mg–Si bonding. Tani and Kido[15] have reported the structural, elastic, and thermodynamic properties of this material at zero pressure. Several recent studies have reported the ZT value of Mg_2Si and its solid solutions. Zaitsev *et al.*[16] achieved a maximum ZT of 1.1 within the

*Project supported by the Council of Scientific & Industrial Research (CSIR), India.

†Corresponding author. E-mail: kulwinderphysics@gmail.com

© 2016 Chinese Physical Society and IOP Publishing Ltd

temperature range of 300–870 K. Isoda *et al.*[17] achieved a maximum ZT, 1.2 at 620 K. Jung and Kim obtained ZT= 0.7 at 830 K with Bi-doped Mg_2Si.[18] Kyung–Ho *et al.*[19] obtained maximum ZT= 0.24 at 773 K. Mao *et al.*[20] have experimentally reported that at 7.5 GPa, the cubic antiflourite structure changes into an anti-cotunnite structure. Yu *et al.*[21] reported the electronic, elastic, and thermal properties (entropy and specific heat) of Mg_2Si at different pressures and temperatures. With the first-principles calculation, Yu *et al.*[22] reported the metallization of Mg_2Si takes place at 8 GPa. They also found that the phase transformation from antiflourite to anti-cotunnite structure takes place at 8.38 GPa. Hao *et al.*[23] and Hao[24] experimentally revealed that a phase transition takes place at 7.5 GPa. Murtaza *et al.*[25] reported the effect of pressure on the electronic properties of this material. To the best of our knowledge, the thermoelectric properties such as the Seebeck coefficient, electrical and thermal conductivity, etc., of Mg_2Si at different pressures and at high temperature has not yet been reported.

Therefore, the aim of this study is mainly devoted to predict the evolution of electronic and thermoelectric properties of Mg_2Si under pressure to fill the lack of experimental data. The rest of the paper is divided into three sections. In Section 2, the computational methodology used in the present calculations is briefly explained. In Section 3, the results of electronic and thermoelectric properties of the material are discussed. Section 4 briefly summarizes the whole paper.

2. Theoretical and computational methodology

Mg_2Si is the face-centered cubic (FCC) structure. Its corresponding space group is $Fm\text{-}3m$.[26] It belongs to the antifluorite structure family. There are three in-equivalent sites that can be specified in the irreducible unit cell, namely Si: $a(0,0,0)$, Mg: $a(1/4,1/4,1/4)$, and Mg: $a(1/4,1/4,3/4)$. In these calculations, $2\times1\times1$ super cell of Mg_2Si which contains 24 atoms (16 Mg atoms and 8 Si atoms) has been constructed.

In this study, we adopted the same methodology which we have used to find the electronic and thermoelectric properties of Mg_2C.[27] The electronic structure calculations were performed using density functional theory (DFT) based on the plane wave pseudo potential method as implemented in the Quantum Espresso package.[28] The generalized gradient approximation (GGA)[29] of Perdue–Burke–Ernzerhof (PBE) was used for the exchange–correlation functional. The cutoff for the kinetic energy was set to 40 Ry (1 Ry = 13.6056923 eV) for the plane-wave expansion of the electronic wave functions. The charge-density cutoff was kept at 400 Ry and the Marzari-Vanderbilt cold smearing size was fixed at 0.003 Ry. The Brillouin zone integration was performed using the Monkhorst–Pack scheme[30] with $4\times8\times8$ meshes. The lattice constant of Mg_2Si was optimized until the total energy converged to at least 10^{-6} Ry, and the forces between atoms became smaller than 10^{-4} Ry/bohr. For the density of state (DOS) calculation, we used the tetrahedron method with $16\times16\times16$ denser k-point mesh.

We have interfaced the Quantum Espresso package with the BoltzTraP code[31] to calculate the thermoelectric properties. The BoltzTraP code is based on the Boltzmann theory and calculates various band structure dependent quantities such as electrical conductivity (σ) and electronic thermal conductivity (k_e) within constant time approximation and rigid band approximation (RBA).[32,33] The BoltzTraP code can analytically represent these band energies with a smoothed Fourier interpolation and thereafter we can obtain the necessary derivatives such as electron velocities for transport properties. The electrical conductivity (σ) and seebeck coefficient (S) as a function of group velocity (v_α) is expressed as

$$\sigma_{\alpha\beta}(\varepsilon)=\frac{e^2}{N}\sum_{i,k}\tau v_\alpha(i,k)\frac{\delta(\varepsilon-\varepsilon_{i,k})}{\mathrm{d}\varepsilon}, \tag{3}$$

where N, τ, ε, α, and β, $v_\alpha(i,k)$ are the number of k points sampled, relaxation time, band energy, tensor indices, and a component of the group velocities respectively. Further, the group velocity can be written as

$$v_\alpha(i,k)=\frac{1}{\hbar}\frac{\partial\varepsilon_{i,k}}{\partial k_\alpha}. \tag{4}$$

The transport coefficients are a function of temperature and chemical potential and can be calculated by integrating the transport distribution[32]

$$\sigma_{\alpha\beta}(T;\mu)=\frac{1}{\Omega}\int\sigma_{\alpha\beta}(\varepsilon)\left[-\frac{\partial f_\mu(T;\varepsilon)}{\partial\varepsilon}\right]\mathrm{d}\varepsilon, \tag{5}$$

$$\upsilon_{\alpha\beta}(T;\mu)=\frac{1}{eT\Omega\sigma_{\alpha\beta}(T,\mu)}\int\sigma_{\alpha\beta}(\varepsilon)(\varepsilon-\mu)\times\left[-\frac{\partial f_\mu(T;\varepsilon)}{\partial\varepsilon}\right]\mathrm{d}\varepsilon, \tag{6}$$

$$S_{ij}=E_i(\nabla_jT)^{-1}=(\sigma^{-1})\alpha_i\upsilon_{\alpha j}, \tag{7}$$

$$\kappa^0_{\alpha\beta}(T;\mu)=\frac{1}{e^2T\Omega}\int\sigma_{\alpha\beta}(\varepsilon)(\varepsilon-\mu)^2\left[-\frac{\partial f_\mu(T;\varepsilon)}{\partial\varepsilon}\right]\mathrm{d}\varepsilon, \tag{8}$$

where e, k^0, Ω, μ, and f_μ are the electronic charge, the electronic part of thermal conductivity, volume of unit cell, chemical potential, and Fermi–Dirac distribution function respectively.

The electrical conductivity (σ) is expressed in terms of the ratio of σ/τ. To calculate the electrical conductivity of the system, we must determine the relaxation time. Hence, we adopted the strategy previously used by Ong *et al.*[34] and Zou *et al.*[35] We assumed that the relaxation time is direction independent, and treated the relaxation time as constant for certain specific temperature and carrier concentration. The reported experimental electrical resistivity (ρ) for Mg_2Si is

7.14×10^{-2} Ω·cm[36] at 300 K, which combined with the calculated σ/τ yields $\tau = 0.176 \times 10^{-14}$ s for this sample. By inserting these values into the standard electron phonon relaxation time equation ($\tau = CT^{-1}n^{-1/3}$), the value of constant $Cn^{-1/3}$ is determined as 5.28×10^{-13} s·K. Further, using this value, we calculate electrical conductivity σ.

In this study, we used the ShengBTE code[37] to calculate the lattice thermal conductivity, which is based on the phonon Boltzmann transport equation (pBTE). This code is based on the second-order (harmonic) and third-order (an harmonic) interatomic force constants (IFCs) combined with a full solution of the pBTE and can successfully predict the k_l.[38,39] We calculated the second-order (harmonic) interatomic force constants (IFCs) from the Quantum Espresso package[28] and the third-order (an harmonic) interatomic force constants (IFCs) was obtained from ShengBTE.[37]

The lattice parameter and bulk modulus have been calculated by computing the total energy for different volumes and fitted to Murnaghan's equation of state[40]

$$P(V) = \frac{B_0}{B_0'}\left[\left[\frac{V}{V_0}\right]^{-B_0'} - 1\right], \tag{9}$$

where P is the pressure, V_0 is the reference volume, V is the deformed volume, B_0 is the bulk modulus, and B_0' is the derivative of the bulk modulus with respect to pressure.

3. Results and discussion

3.1. Electronic properties

The calculated lattice constant, bulk modulus, and band gap at different pressures are summarized in Table 1. The calculated lattice constant of Mg_2Si at zero pressure is 6.364 Å. This value is close to the previous theoretical result reported by Pandit *et al.*[41] and experimental observation by Fan *et al.*[42] The calculated values of the lattice constant at all pressures are in excellent agreement with the theoretical data. The calculated band structure and density of states (DOS) of Mg_2Si at different pressures are shown in Figs. 1 and 2, respectively. It is clear from the figure that Mg_2Si is an indirect band gap semiconductor at all applied pressures. The highest occupied valance band (HOVB) lies on the Γ point, and the lowest unoccupied conduction band (LUCB) is at X high symmetry point. Overall, the feature of our band structure at zero pressure shows a good agreement with the data reported by Boulet *et al.,*[43] but is underestimated as compared to the experimental value. The standard local density approximation (LDA) and generalized gradient approximation (GGA) functional have their own limitations. Note that the LDA or GGA provides a smaller band gap than the experimental value due to the well-known underestimation of the conduction band state energies in the DFT calculation.[44] The band structures are quite similar at all pressures. Only the band gap reduces with pressure. The valence band is divided into two sub bands. Starting from the lower energy band, these energy bands consist of Si 3s states. The second bands of the valence band are mainly due to Si p states and the small contribution of Mg s and p states. In the conduction band, both the Si and Mg contributions were nearly the same. The conduction bands are a mix of Mg s, p states and Si s, p states. The valance bands have a stronger Si p character. This is clearly shown in the PDOS depicted in Fig. 3. Moving upward in energy, at all pressures there is a distinct energy gap. With the increase in pressure, the valence band energy level decreases and the valence band width increases. From the calculated band structures and DOS, we can derive that the system is changing from semiconductor to metallic with the increase in pressure.

Table 1. Calculated lattice constant, band gap, and bulk modulus at different pressures and comparison with available experimental and theoretical data.

At $P = 0$ GPa	Properties	Calculated (this work)	Previous theoretical work	Experimental work
	lattice constant/Å	6.364	6.3690,[41] 6.34[45]	6.35,[46] 6.37[42]
	band gap/eV	0.21	0.42,[41] 0.21[43]	0.37,[11] 0.78[12]
	bulk modulus/GPa	55.4	54,[41] 56.49[47]	52.5,[43] 57.03[23]
At $P = 2$ GPa	Properties	Calculated (this work)	Previous theoretical work	Experimental work
	lattice constant/Å	6.328	6.313[21]	–
	band gap/eV	0.176	–	–
	bulk modulus/GPa	59.2	60.6[21]	–
At $P = 4$ GPa	Properties	Calculated (this work)	Previous theoretical work	Experimental work
	lattice constant/Å	6.263	6.248[21]	–
	band gap/eV	0.139	–	–
	bulk modulus/GPa	67.1	68.0[21]	–
At $P = 6$ GPa	Properties	Calculated (this work)	Previous theoretical work	Experimental work
	lattice constant/Å	6.210	6.190[21]	–
	band gap/eV	0.104	–	–
	bulk modulus/GPa	73.8	75.4[21]	–

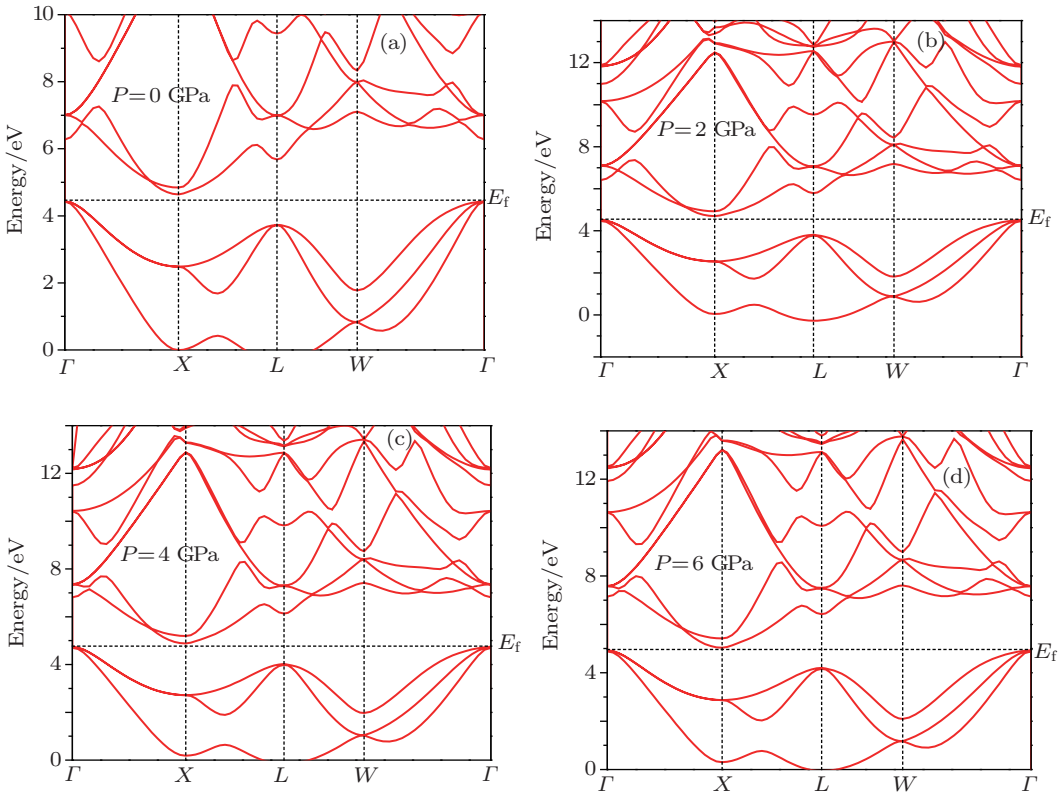


Fig. 1. (color online) Electronic band structures of Mg_2Si at different pressures. (a) $P = 0$ GPa, (b) $P = 2$ GPa, (c) $P = 4$ GPa, and (d) $P = 6$ GPa.

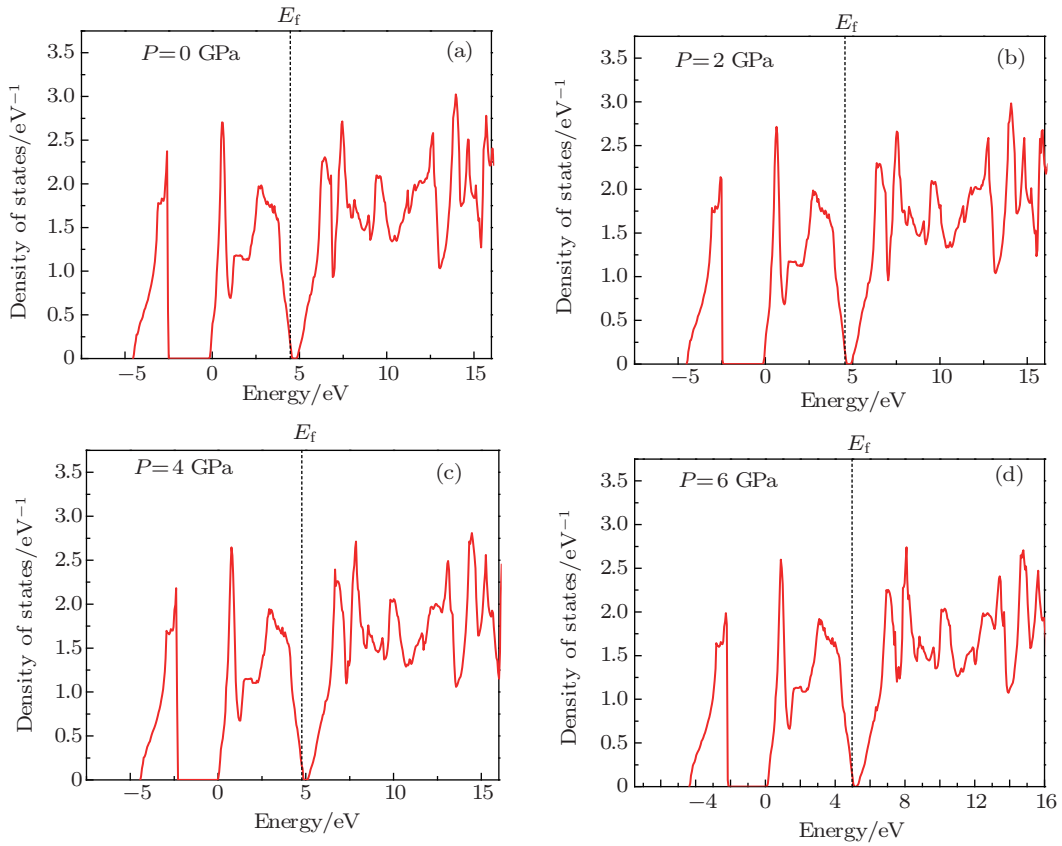


Fig. 2. (color online) Density of states of Mg_2Si at different pressures. (a) $P = 0$ GPa, (b) $P = 2$ GPa, (c) $P = 4$ GPa, and (d) $P = 6$ GPa.

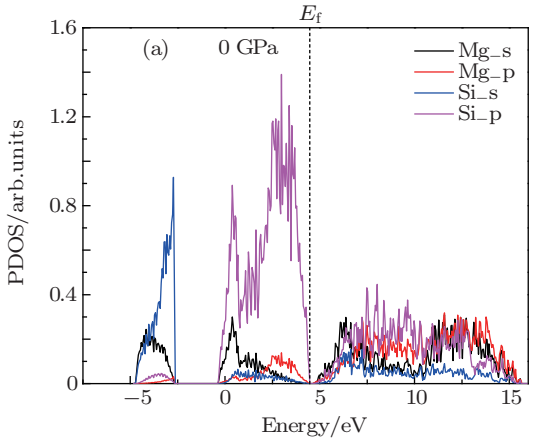


Fig. 3. (color online) Projected density of state of Mg_2Si at zero pressure.

3.2. Thermoelectric properties

The variation of Seebeck coefficient (S), the electrical conductivity (σ/τ), the electronic thermal conductivity (k_e/τ), and power factor ($S^2\sigma/\tau$) with respect to temperature are shown in Fig. 4. The Seebeck coefficient increases with temperature and at high temperature it decreases with the increase in temperature due to the presence of thermally excited minority carriers which increase the electronic concentration (n). We know that the seebeck coefficient and carrier concentration are related to each other as follows:

$$S = \frac{8\pi^2 k_b^2}{3eh^2} m^* T \left[\frac{\pi}{3n}\right]^{2/3}, \tag{10}$$

where k_b is the Boltzmann constant, m^* is effective mass, and n denotes the carrier concentrations. According to Eq. (10), the Seebeck coefficient is inversely proportional to the carrier concentration. At zero pressure, the increasing in Seebeck coefficient with temperature is due to a low concentration of charge carriers and at high temperature it decreases due to the increase of thermally excited electrons. The negative sign of the Seebeck coefficient indicates that Mg_2Si is an n-type semiconductor, i.e., conduction is due to electrons. It is also seen that with the increase in pressure, the Seebeck coefficient decreases. As shown in Table 1, with the increase in pressure, the band gap decreases and the system goes towards a metallic nature, which results in an increased effective mass. The increase in effective mass affects the thermoelectric properties. Kalarasse and Bennecer[48] reported that Mg_2Si became metallic at 6.1 GPa.

Figure 4(b) shows the variation of electrical conductivity (σ/τ) with temperature. The figure shows that the electrical conductivity increases with the increase in temperature which shows the semiconductor behavior[49] of this compound. The electrical conductivity increases due to the increase in the number of charge carriers at high temperature. The relation between the electrical conductivity and carrier concentration (n) is given as

$$\sigma = ne\mu, \tag{11}$$

where e is the electronic charge and μ is the mobility. The positive temperature dependence of electrical conductivity at high temperature is due to an increase in carrier concentration. Our calculation at zero pressure shows reasonable agreement with data reported by Fu *et al.*[50]

Figure 4(c) shows the variation of electronic thermal conductivity with temperature. The electronic contribution of thermal conductivity directly depends upon carrier concentration, according to the following equation:

$$k_e = \frac{n\pi^2 T k_b^2}{3m^* v_e}. \tag{12}$$

With the increase in pressure, there is no change in carrier concentration, so the electronic thermal conductivity remains constant at all pressures.

Figure 4(d) shows the variation of power factor (PF) with temperature. As the temperature increases, the power factors at all pressures increase and reach the maximum value at 800 K. However, with the increase in pressure, the PF decreases.

From the above discussion, we conclude that with an increase in pressure, the power factor of Mg_2Si decreases. Power factor is an accumulated effect of Seebeck coefficient and electrical conductivity. With the increase in pressure, the band gap decreases which decreases the effective mass of electron. The Seebeck coefficient directly depends upon the effective mass, thus reduces the effective mass, decreases the Seebeck coefficient, and increases the electrical conductivity. Here, the Seebeck coefficient plays the main role in decreasing the power factor.

Figure 5 shows the variation of electronic thermal conductivity and lattice thermal conductivity with varied temperature at zero pressure. This figure shows that the electronic part of thermal conductivity also increases with the increase in temperature. The lattice contribution of thermal conductivity decreases with the increase in temperature. Figure 6 shows the variation of total thermal conductivity (k) with temperature at zero pressure. The observed value of total thermal conductivity decreases with the increase in temperature. Our calculated results show a good agreement with data reported by Tani *et al.*[51] and Akasaka *et al.*[7] In this calculation, we find that 99% thermal conductivity is due to the lattice contribution. The lattice contribution of thermal conductivity has a more profound role than the electronic contribution of thermal conductivity. The total thermal conductivity results from the lattice contribution at all temperatures. This is due to the low carrier concentration.

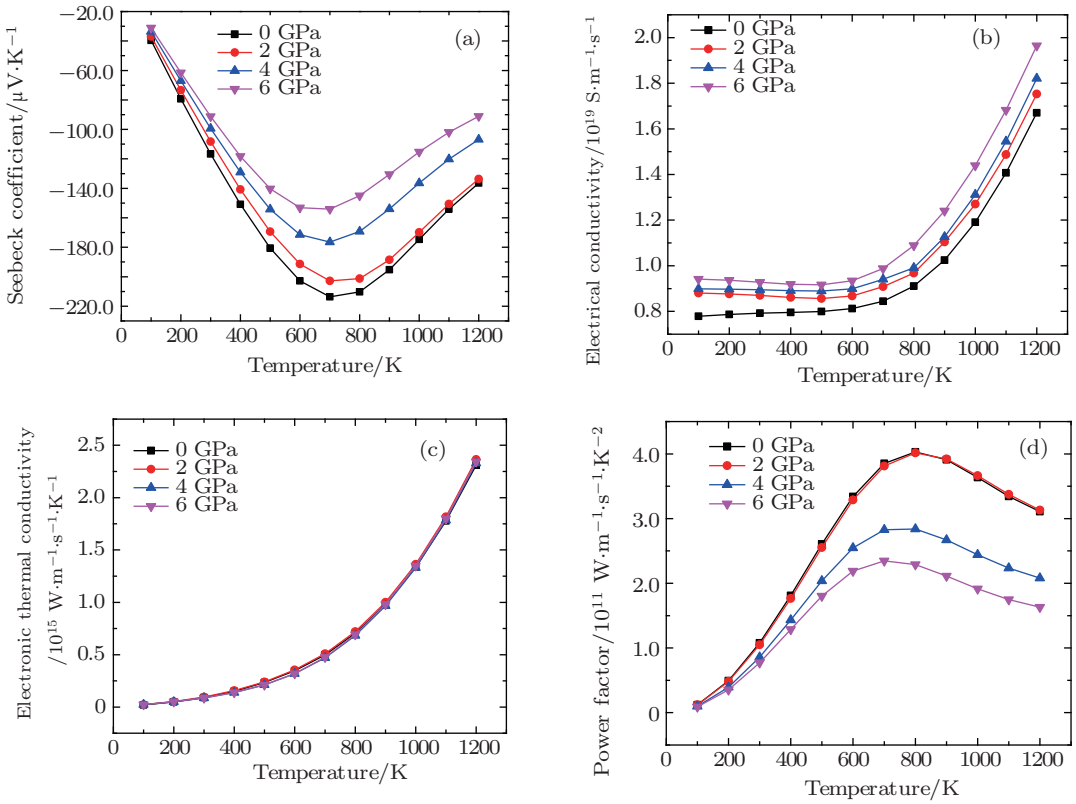


Fig. 4. (color online) (a) Seebeck coefficient (S), (b) electrical conductivity (σ/τ), (c) electronic thermal conductivity (k_e/τ), and (d) power factor ($S^2\sigma/\tau$) versus temperature at different pressures.

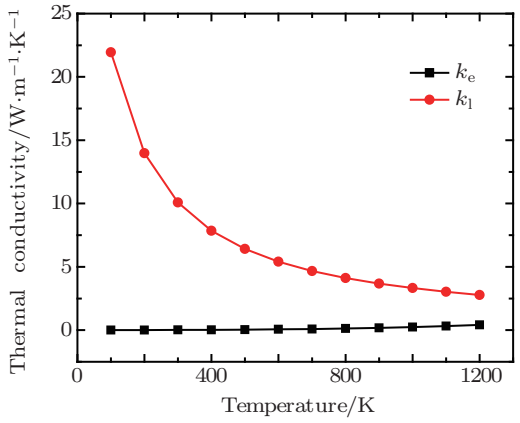


Fig. 5. (color online) Electronic (k_e) and lattice (k_l) thermal conductivity versus temperature at zero pressure.

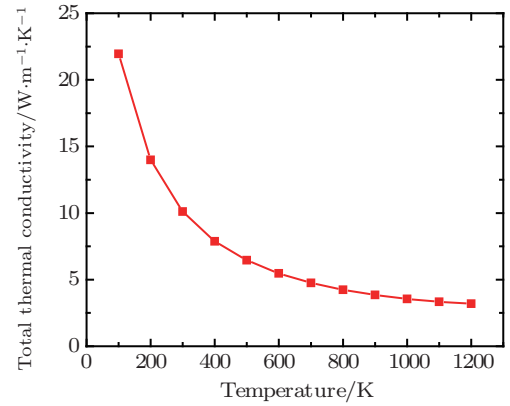


Fig. 6. (color online) Variation of total thermal conductivity with temperature at zero pressure.

Figure 7 shows the variation figure of merit (ZT) with temperature at normal pressure. The figure of merit for Mg_2Si was low due to the low electrical conductivity, i.e., low carrier concentration. Mg_2Si attained the maximum value of ZT=0.0018 at 1000 K.

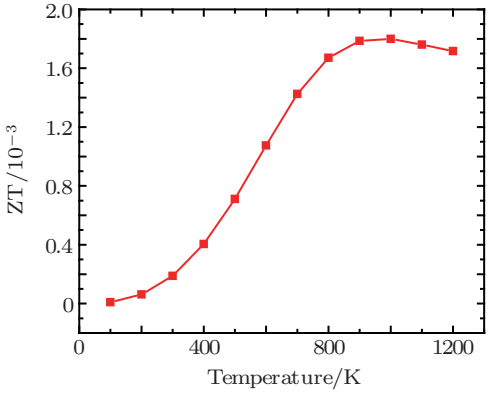


Fig. 7. (color online) Figure of merit (ZT) versus temperature at zero pressure.

4. Conclusion

We have used the density functional theory with GGA to investigate the effect of pressure on the electronic and thermoelectric properties of Mg_2Si. The results show that the band gap decreases with pressure. Instead of electronic properties, overall thermoelectric properties decrease with pressure. The Seebeck coefficient and power factor decrease with pressure but electrical conductivity increases with pressure. The total

thermal conductivity at normal pressure decreases with temperature and the maximum value of figure of merit is 0.0018 at 1000 K.

Acknowledgment

Authors are thankful to the Bioinformatics & Computational Biology (SCFBio), and the Department of Biotechnology, IIT Delhi, for providing the supercomputing facility.

References

[1] Wood C 1988 *Rep. Prog. Phys.* **51** 459
[2] Liu Z, Watanabe M and Hanabusa M 2001 *Thin Solid Films* **381** 262
[3] Borisenko V E 2000 *Semiconducting Silicides* (Springer-Verlag) p. 285
[4] Morris R G, Redin R D and Danielson G C 1958 *Phys. Rev.* **109** 1909
[5] Akasaka M, Iida T, Matsumoto A, Yamanaka K, Takanashi Y, Imai T and Hamada N 2008 *J. Appl. Phys.* **104** 013703
[6] Yu Z, Xie Q, Xiao Q and Zhao K 2009 *Acta Phys. Sin.* **58** 6889 (in Chinese)
[7] Li C, Wu Y, Li H and Liu X 2009 *J. Alloys Compd.* **477** 212
[8] Wang X N, Wang Y, Zou J, Zhang T C, Mei Z X, Guo Y and Zhang Z 2009 *Chin. Phys. B* **18** 3079
[9] Bashenov V K, Mutal A M and Timofeenko V V 1978 *Phys. Status Solidi B* **87** 77
[10] Aizawa T and Song R 2006 *Intermetallics* **14** 382
[11] DiSalvo F J 1999 *Science* **285** 703
[12] Snyder G J and Ursell T S 2003 *Phys. Rev. Lett.* **91** 148301
[13] Baranek P, Schamps J and Noiret I 1997 *J. Phys. Chem. B* **101** 9147
[14] Baranek P and Schamps J 1999 *J. Phys. Chem. B* **103** 2601
[15] Tani J I and Kido H 2008 *Comput. Mater. Sci.* **42** 531
[16] Zaitsev V K, Fedorov M I, Gurieva E A, Eremin I S, Konstantinov P P, Samunin A Y and Vedernikov M V 2006 *Phys. Rev. B* **74** 045207
[17] Isoda Y, Tada S, Nagai T, Fujiu H and Shinohara Y 2010 *Mater. Trans.* **51** 868
[18] Jung J Y and Kim I H 2010 *Electron. Mater. Lett.* **6** 187
[19] Kim K H, Choi S M and Seo W S 2010 *J. Korean Phy. Soc.* **57** 1072
[20] Mao H K, Xu J and Bell P M 1986 *J. Geophys. Res.* **91** 4673
[21] Yu B, Chen D, Tang Q, Wang C and Shi D 2010 *J. Phys. Chem. Solids* **71** 758
[22] Yu F, Sun J X, Yang W, Tian R G and Ji G F 2010 *Solid State Commun.* **150** 620
[23] Hao J, Zou B, Zhu P, Gao C, Li Y, Liu D and Zou G 2009 *Solid State Commun.* **149** 689
[24] Hao J 2008 *Studies on the Characteristics and Structure Transformation of Magnesium Silicide under High Pressure* (Jilin University)
[25] Murtaza G, Sajid A, Rizwan M, Takagiwa Y, Khachai H, Jibran M and Omran S B 2015 *Mat. Sci. Semiconduct. Process.* **40** 429
[26] Ziman J M 2001 *Electrons and Phonons Oxford Classics Series* (Oxford: Clarendon Press)
[27] Kulwinder K and Ranjan K 2016 *Chin. Phys. B* **25** 26402
[28] Giannozzi P, Baroni S, Bonini N, Calandra M, Car R, Cavazzoni C, Ceresoli D, Chiarotti G L, Cococcioni M, Dabo I, Corso A D, Gironcoli S de, Fabris S, Fratesi G, Gebauer R, Gerstmann U, Gougoussis C, Kokalj A, Lazzeri M, Martin-Samos L, Marzari N, Mauri F, Mazzarello R, Paolini S, Pasquarello A, Paulatto L, Sbraccia C, Scandolo S, Sclauzero G, Seitsonen A P, Smogunov A, Umari P and Wentzcovitch R M 2009 *J. Phys.: Conden. Matter* **21** 395502
[29] Perdew J P, Burke K and Ernzerhof M 1996 *Phys. Rev. Lett.* **77** 3864
[30] Monkhorst H J and Pack J D 1976 *Phys. Rev. B* **13** 5188
[31] Madsen G K and Singh D J 2006 *Comput. Phys. Commun.* **175** 67
[32] Scheidemantel T J, Ambrosch-Draxl C, Thonhauser T, Badding J V and Sofo J O 2003 *Phys. Rev. B* **68** 125210
[33] Jodin L, Tobola J, Pecheur P, Scherrer H and Kaprzyk S 2004 *Phys. Rev. B* **70** 184207
[34] Ong K P, Singh D J and Wu P 2011 *Phys. Rev. B* **83** 115110
[35] Zou D F, Xie S H, Liu Y Y, Lin J G and Li J Y 2013 *J. Appl. Phys.* **113** 193705
[36] Tani J I and Kido H 2007 *Intermetallics* **15** 120237
[37] Li W, Carrete J, Katcho N A and Mingo N 2014 *Comput. Phys. Commun.* **185** 1747
[38] Ma J, Li W and Luo X 2014 *Appl. Phys. Lett.* **105** 082103
[39] Carrete J, Mingo N and Curtarolo S 2014 *Appl. Phys. Lett.* **105** 101907
[40] Munrnaghan F D 1944 *Proc. Natl. Acad. Sci. USA* **30** 244
[41] Pandit P and Sanyal S P 2011 *Indian Journal of Pure and Applied Physics* **49** 692
[42] Fan W, Chen R, Wang L, Han P and Meng Q 2011 *J. Electron. Mater.* **40** 1209
[43] Boulet P, Verstraete M J, Crocombette J P, Briki M and Record M C 2011 *Comput. Mater. Sci.* **50** 847
[44] Gunnarsson O and Schönhammer K 1986 *Phys. Rev. Lett.* **56** 1968
[45] Poopanya P and Yangthaisong A 2013 *Physics of Semiconductors: Proceedings of the* 31*st International Conference on the Physics of Semiconductors* 2012 p. 415 (AIP Publishing)
[46] You S W and Kim I H 2011 *Curr. Appl. Phys.* **11** 392
[47] Corkill J L and Cohen M L 1993 *Phys. Rev. B* **48** 17138
[48] Kalarasse F and Bennecer B 2008 *J. Phys. Chem. Solids* **69** 1775
[49] Clark C R, Wright C, Suryanarayana C, Baburaj E G and Froes F H 1997 *Mat. Lett.* **33** 71
[50] Fu G, Zuo L, Longtin J, Nie C and Gambino R 2013 *J. Appl. Phys.* **114** 144905
[51] Tani J I and Kido H 2007 *Intermetallics* **15** 1202